



Editor Choice Paper

Synthesis and characterization of new rhodium and iridium complexes with trianisylphosphine, PAn_3 , and evaluation of their catalytic behavior in the homogeneous hydrogenation of cinnamaldehyde

Vanessa R. Landaeta^{a,*}, Francisco López-Linares^b, Roberto Sánchez-Delgado^c, Claudio Bianchini^d, Fabrizio Zanobini^d, Maurizio Peruzzini^{d,*}

^a Universidad Simón Bolívar, Departamento de Química, Valle de Sartenejas, Baruta, Aptdo. 89000, Caracas 1080-A, Venezuela

^b Schulich School of Engineering, University of Calgary, Alberta, Canada

^c Chemistry Department, Brooklyn College and The Graduate Center of The City University of New York, Brooklyn, NY 11210, USA

^d Istituto di Chimica dei Composti Organometallici (ICCOM-CNR), Via Madonna del Piano 10, Polo Scientifico, 50019 Sesto Fiorentino (FI), Italy

ARTICLE INFO

Article history:

Received 16 September 2008

Accepted 11 November 2008

Available online 21 November 2008

Keywords:

Hydrogenation

Trans-cinnamaldehyde

Iridium and rhodium complexes

Stereoelectronic properties

Phosphines

ABSTRACT

A new family of rhodium and iridium compounds with the bulky tris(*ortho*-methoxyphenyl) phosphine (PAn_3) was synthesized and characterized by NMR methods. The X-ray crystal structures of $\text{RhCl}(\text{PAn}_3)(\text{COD})$ (**1**) and $\text{Ir}[(\text{PBz}_3)(\text{PAn}_3)(\text{COD})]\text{PF}_6$ (**4**) have been determined. A stabilizing agostic interaction has been crystallographically observed in both compounds, due to the steric hindrance of the *ortho*-substituted phosphine ligand and its presence has been associated to the fluxional behavior shown by the complexes on the NMR timescale in solution. Iridium complexes containing PBz_3 and/or PAn_3 have been evaluated as catalyst precursors for the hydrogenation of *trans*-cinnamaldehyde (CNA), and their activities have also been compared to those of other iridium complexes containing bulky phosphine ligands, such as PTol_3 (tris-*ortho*-tolyl-phosphine). The catalytic experiments show that irrespectively of the phosphine combination, all of the evaluated catalysts prevalently hydrogenate the C=C moiety. However, the product selectivity can be tuned by changing either the substrate/catalyst ratio or the phosphine ligand at the metal center. The catalyst with PAn_3 proved to be more efficient and also gave higher yields of the enol product, indicating that stereoelectronic effects are responsible for the changes in selectivity.

© 2008 Elsevier B.V. All rights reserved.

1. Introduction

The decoration of phenyl rings with different substituents in aromatic phosphine ligands has become one of the most effective ways to tune the electronic and steric properties of these ligands and to get the most out of catalytic systems [1,2]. Methoxy (OCH_3) substituents have played a major role in these modifications [2–9], specially when these are performed in *ortho* position, since they can electronically tune the properties of the ligand as well as create important steric effects.

Several reports [3–8] have appeared regarding the coordination chemistry of methoxyphenyl phosphines with more than one substituent in the aromatic ring. As an example, it is worth mentioning the in-depth studied family of ligands derived from 2,6-dimethoxyphenyl groups, MDMPP, BDMPP and TDMPP [3–6] (Fig. 1), which show multiple hapticity since the coordination may

occur not only through the phosphorus atom, but also through at least one of the oxygen atoms from the methoxy groups [4,6]. Also, low coordination numbers can be stabilized using this kind of ligands as well as the more encumbering trisubstituted TMPP [6].

Chiral methoxyphenyl phosphine ligands have been reported [7,8] and among these, DIPAMP (Fig. 1) is the most successful case [7]. Also, interesting synthetic methodologies have been developed to obtain methoxy-substituted phosphine ligands with polar groups [9]. However, regardless of the interesting properties observed with these ligands, the simpler tris(*ortho*-methoxyphenyl)phosphine, hereafter tris(*ortho*-anisyl)phosphine (PAn_3), has received only little attention [10–14]. Among miscellaneous results, comparative studies on the basicity of PAn_3 and other phosphines have been carried out by evaluating the formation of ionic pairs of gallium (III) with PR_3 [10]. The reactivity of a number of tertiary phosphine ligands, including PAn_3 , towards $(\text{Ph}_2\text{Se}_2\text{I}_2)_2$ has been reported [11] while some (*ortho*-anisyl)phosphides were also described [12].

The coordination chemistry of PAn_3 has attracted scarce attention, essentially confined to $\text{M}(\text{CO})_6$ derivatives ($\text{M} = \text{Cr}, \text{Mo}, \text{W}$)

* Corresponding author. Tel.: +58 212 9063984; fax: +58 212 9063961.

E-mail addresses: vlandaeta@usb.ve (V.R. Landaeta), mperuzzini@iccom.cnr.it (M. Peruzzini).

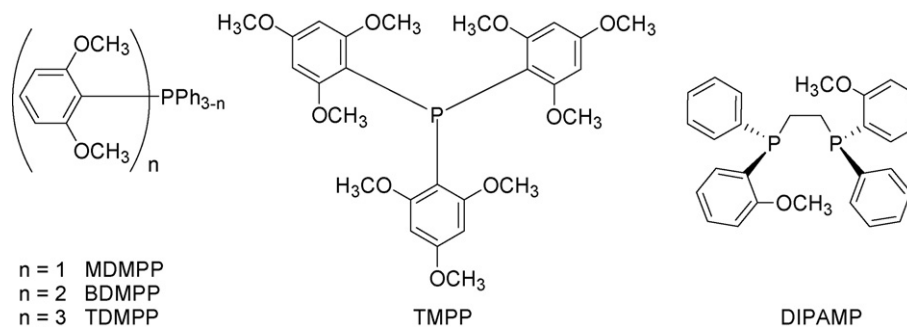


Fig. 1. Examples of methoxyphenylphosphines from the literature [4,6,7].

[13] and gold complexes [14]. To the best of our knowledge, only one rhodium(I) compound with PAN_3 , namely $\text{RhCl}(\text{PAN}_3)(\text{COD})$, COD = 1,5-cyclo-octadiene, has been briefly described [15] without any crystallographic data. Also, one Rh(II) species containing PAN_3 has been reported [16]. In contrast, no iridium/ PAN_3 complex has been mentioned and no catalytic study involving PAN_3 complexes has been reported.

Herein, we report the synthesis and characterization of a family of rhodium and iridium complexes with tris(*ortho*-anisyl)phosphine (PAN_3) and describe the solid state structure of two exemplificative species like $\text{RhCl}(\text{PAN}_3)(\text{COD})$ and $[\text{Ir}(\text{PBz}_3)(\text{PAN}_3)(\text{COD})]\text{PF}_6$. The catalytic properties of some of these species in the hydrogenation of *trans*-cinnamaldehyde (CNA) have also been studied, since the production of allylic alcohols like cinnamyl alcohol or cinnamol has importance due to their potential use as building blocks in organic synthesis [17]. Finally, a comparison of the catalytic properties of Ir/ PAN_3 precursors with respect to other complexes bearing other bulky phosphine ligands, such as PBz_3 [18] or PTol_3 is reported.

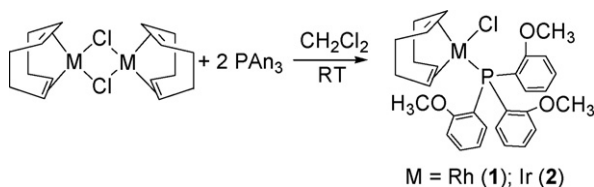
2. Results and discussion

2.1. Synthesis and characterization of $\text{MCl}(\text{PAN}_3)(\text{COD})$ ($\text{M} = \text{Rh}$, Ir)

The binuclear complexes $[\text{MCl}(\text{COD})]_2$ ($\text{M} = \text{Rh}$, Ir) react with two equivalents of PAN_3 under mild conditions (CH_2Cl_2 , room temperature), to give bright yellow crystals of the neutral complexes $\text{MCl}(\text{PAN}_3)(\text{COD})$ [$\text{M} = \text{Rh}$ (**1**), Ir (**2**)] in high yield (>90%) (Scheme 1). Compounds **1** and **2** are air-stable in the solid state and are soluble in polar organic solvents.

An alternative lower yield synthesis of compound **1** has already been reported by Tiburcio et al. [15]. Crystals of **1** suitable for an X-ray diffraction analysis were grown from a dichloromethane/ethanol solution. An ORTEP drawing showing the structure of compound **1** is given in Fig. 2. A summary of crystal data and a selection of bond distances (Å) and angles (°) are collected in Tables 1 and 2.

Complex **1** crystallizes in a monoclinic system with a $P2_1/n$ space group. The molecular structure is a strongly distorted square planar one, reflecting the presence of the bulky phosphine ligand. The



Scheme 1.

Table 1

Summary of Crystal Data for $\text{RhCl}(\text{PAN}_3)(\text{COD})$ (**1**) and $[\text{Ir}(\text{PBz}_3)(\text{PAN}_3)(\text{COD})]\text{PF}_6$ (**4**).

	1	4
Formula	$\text{RhC}_{29}\text{H}_{33}\text{ClO}_3$	$\text{C}_{50}\text{H}_{54}\text{F}_6\text{IrO}_3\text{P}_3$
Mol. wt.	598.88	1102.04
Cryst size (mm)	$0.65 \times 0.35 \times 0.45$	$0.52 \times 0.20 \times 0.13$
Cryst. syst.	Monoclinic	Triclinic
Space group	$P2_1/n$	P_{-1}
<i>a</i> (Å)	8.559 (3)	10.1516 (19)
<i>b</i> (Å)	18.046 (2)	20.521 (4)
<i>c</i> (Å)	17.004 (3)	24.595 (3)
β (degree)	90.144 (19)	100.728 (14)
<i>V</i> (Å ³)	2626.4(11)	5034.1 (16)
<i>Z</i>	4	4
<i>d</i> _{calc} (mg/m ³)	1.515	1.454
Abs. coeff. (mm ⁻¹)	0.842	2.808
<i>F</i> (000)	1232	2216
θ range (degree)	2.26–24.97	2.04–22.98
Index ranges	$-10 \leq h \leq 10$ $0 \leq k \leq 21$ $0 \leq l \leq 20$	$-11 \leq h \leq 10$ $0 \leq k \leq 22$ $0 \leq l \leq 27$
Tot. number of data	4778	7152
Number of unique data, $I \geq 2\sigma(I)$	4617 [<i>R</i> (int)=0.0196]	6966
<i>S</i> (goodness of fit on <i>F</i> ²)	1.024	0.851
<i>R</i> 1 ($I \geq 2\sigma(I)$)	0.0310	0.0481
<i>wR</i> 2 (all)	0.0700	0.1317
Largest diff. peak and hole (e/Å ³)	0.339, –0.334	1.290, –0.773

Table 2

Selected bond distances (Å) and angles (°) for $\text{RhCl}(\text{PAN}_3)(\text{COD})$ (**1**) and $[\text{Ir}(\text{PBz}_3)(\text{PAN}_3)(\text{COD})]\text{PF}_6$ (**4**).

	1	4	
Bond distances			
Rh(1)–C(1)	2.108(3)	Ir(1)–C(4)	2.189(10)
Rh(1)–C(2)	2.131(3)	Ir(1)–C(2)	2.211(10)
Rh(1)–C(3)	2.156(4)	Ir(1)–C(3)	2.193(11)
Rh(1)–C(4)	2.184(4)	Ir(1)–C(1)	2.212(11)
Rh(1)–P(1)	2.3548(9)	Ir(1)–P(2)	2.349(3)
Rh(1)–Cl(1)	2.3803(11)	Ir(1)–P(1)	2.361(2)
Bond angles			
P(1)–Rh(1)–Cl(1)	89.25(4)	C(4)–Ir(1)–C(2)	89.0(4)
C(1)–Rh(1)–C(2)	38.11(15)	C(4)–Ir(1)–C(3)	35.5(4)
C(1)–Rh(1)–C(3)	95.14(16)	C(2)–Ir(1)–C(3)	79.2(4)
C(2)–Rh(1)–C(3)	80.75(15)	C(4)–Ir(1)–C(1)	78.7(5)
C(1)–Rh(1)–C(4)	80.18(16)	C(2)–Ir(1)–C(1)	35.8(5)
C(2)–Rh(1)–C(4)	89.17(15)	C(3)–Ir(1)–C(1)	90.5(5)
C(3)–Rh(1)–C(4)	36.54(17)	C(4)–Ir(1)–P(2)	91.5(3)
C(1)–Rh(1)–P(1)	95.87(10)	C(2)–Ir(1)–P(2)	159.8(4)
C(2)–Rh(1)–P(1)	93.82(10)	C(3)–Ir(1)–P(2)	89.5(3)
C(3)–Rh(1)–P(1)	154.18(15)	C(1)–Ir(1)–P(2)	162.8(4)
C(4)–Rh(1)–P(1)	169.28(14)	C(4)–Ir(1)–P(1)	163.9(4)
C(1)–Rh(1)–Cl(1)	155.69(12)	C(2)–Ir(1)–P(1)	90.3(3)
C(2)–Rh(1)–Cl(1)	165.30(11)	C(3)–Ir(1)–P(1)	159.0(4)
C(3)–Rh(1)–Cl(1)	90.25(12)	C(1)–Ir(1)–P(1)	91.4(3)
C(4)–Rh(1)–Cl(1)	90.45(12)	P(2)–Ir(1)–P(1)	94.67(9)

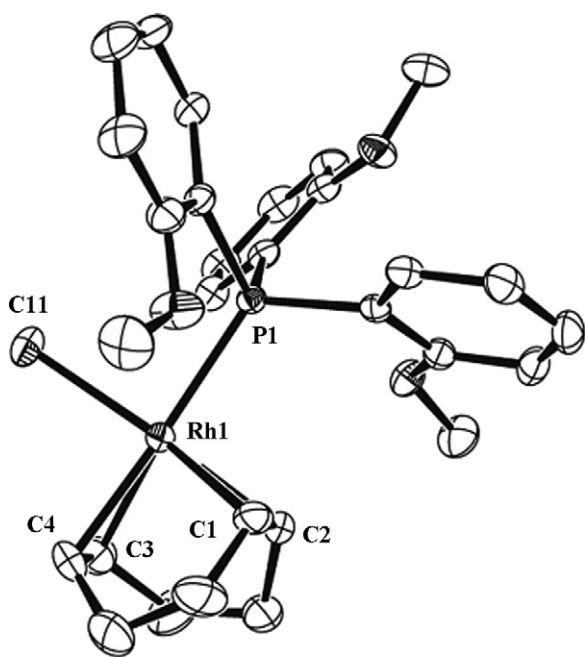


Fig. 2. ORTEP drawing of the complex $\text{RhCl}(\text{PAN}_3)(\text{COD})$ (**1**).

space group is identical to the ones found for the analogous complexes $\text{IrCl}(\text{PBz}_3)(\text{COD})$ previously reported by us [18], and to other analogous $\text{MCl}(\text{PAR}_3)(\text{COD})$ species [19–21]. A variety of Rh(I) and Ir(I) complexes with sterically demanding phosphine ligands (PCy_3 , PPr_3 , PBz_3) exhibit a structure similar to that of compounds **1** and **2** [18–20].

The spectroscopic analysis of compound **1** is in keeping with the data reported in the literature [15]. The $^{31}\text{P}\{^1\text{H}\}$ NMR of **2** in CD_2Cl_2 shows a singlet at 13.34 ppm. The ^1H NMR spectrum of **2** shows a set of 6 signals due to the magnetically inequivalent protons of the COD ligand, two pairs of CH protons and two sets of diastereotopic CH_2 protons. The aromatic protons of the phosphine ligand appear, at room temperature, as one doublet of doublets, two pseudo triplets and one broad signal centered at δ 7.75. As the temperature decreases (Fig. 3), the broad aromatic resonance coalesces while broadening of both the other aromatic resonances and the methoxy groups signal also occurs. At 233 K decoalescence of the aromatic signals occurs with new resonances rising at lower fields and three new methoxy signals are distinguishable. At 183 K the fluxional process is practically frozen and three methoxy singlets have appeared while the originally broad aromatic resonance is resolving into a doublet of doublets. This behavior is attributed to a dynamic process, due to the demanding steric requirements of PAN_3 (cone angle, $\theta = 194^\circ$). The broad aromatic signal observed at room temperature is likely ascribable to one of the *ortho* protons of the phenyl rings in PAN_3 , which owing to the steric congestion approaches the metal thus creating an agostic interaction. At room temperature, fast ligand twisting around the M–P bond, forces one of the three *ortho* protons of PAN_3 to be close to the metal, and results in a fluxional process on the NMR timescale. Lowering the temperature slows down the exchange until at 183 K only one of the three *ortho* protons is close to the metal thus appearing as a doublet of doublets, due to the coupling with both the proton closer to it and the phosphorus atom. This lack of equivalence at low temperatures is confirmed by the resolution of the methoxy signals into three different singlets, one of them at lower fields than the other two which are embedded in a more similar chemical environment. A similar behavior is observed for compound **1** upon variation of the temperature, and can also be confirmed from the solid state

structure of the rhodium analogue in which one of the methoxy groups and one of the *ortho* protons of different phenyl rings are closer to the metal. Selective homonuclear irradiation experiments also confirmed the assignment of each of the protons in species **1** and **2**.

2.2. Reactivity of the neutral complexes $\text{MCl}(\text{PAN}_3)(\text{COD})$ ($\text{M} = \text{Rh}, \text{Ir}$)

Removal of the chloride ligand from **1** or **2** can be readily achieved either by reaction with silver salts in the presence of appropriate ligands or by ligand substitution using an excess of a strong σ -donor such as pyridine (py) in the presence of NH_4PF_6 . Thus, treatment of **1** or **2** dissolved in acetone at room temperature with silver triflate followed by addition of one equivalent of PBz_3 , led to the formation of cationic mixed phosphine ligands derivatives of formula $[\text{M}(\text{PAN}_3)(\text{PBz}_3)(\text{COD})]\text{PF}_6$ [$\text{M} = \text{Rh}$ (**3**); Ir (**4**)] (Scheme 2). Even simpler is the reaction of **1** or **2** with pyridine, which straightforwardly results in the formation of the pyridine adducts $[\text{M}(\text{PAN}_3)(\text{py})(\text{COD})]\text{PF}_6$ [$\text{M} = \text{Rh}$ (**5**); Ir (**6**)] (Scheme 2).

The cationic mixed phosphine ligands **3** and **4** are air and moisture stable solids. Upon reaction of the parent compounds **1** and **2** with Ag^+ and addition of another equivalent of PAN_3 , we were unable to isolate the bis- PAN_3 complexes. It is clear that, in the coordination sphere of rhodium or iridium, the presence of the sterically bulky PAN_3 together with the chelating ligand COD does not allow two very large phosphine ligands to coordinate simultaneously at the Rh(I) or Ir(I) metal centers in *cis*-disposition [21,22]. This consideration may be safely expanded to PCy_3 since, to the best of our knowledge, no bis- PCy_3 has been reported in the literature so far for related square planar derivatives. However, a slightly less bulky ligand such as PBz_3 ($\theta = 165^\circ$), is still able to coordinate to the rhodium

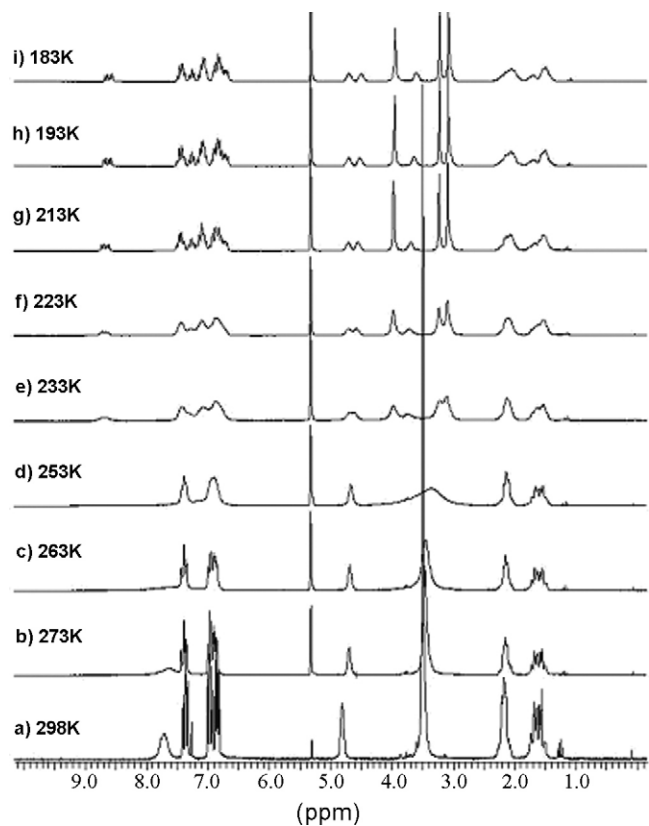
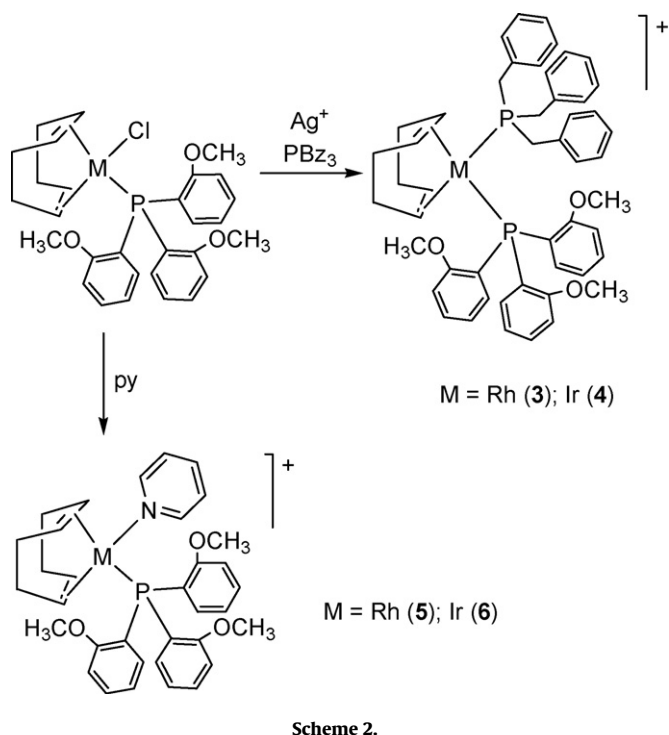


Fig. 3. ^1H NMR spectra of $\text{IrCl}(\text{PAN}_3)(\text{COD})$ (**2**) at variable temperature (200.13 MHz, CD_2Cl_2).



or iridium centers even when a PAN_3 ligand is already bonded to the metal, thus allowing species **3** and **4** to be isolated as stable solid derivatives. Several examples of bis-phosphine cationic Rh(I) or Ir(I) complexes have been reported [18–22].

Species **3** and **4** were completely characterized by both multinuclear NMR spectroscopy and FT-IR. Additionally, for the iridium analogue, crystals suitable for an X-ray diffraction analysis were grown from a diluted dichloromethane/ethanol solution.

As has already been described for the neutral complexes **1** and **2**, a fluxional behavior is observed due to the steric hindrance around the metal center. The $^{31}\text{P}\{^1\text{H}\}$ NMR shows, at room temperature, two broad singlets for **4** and two broad doublets for **3** due to ^{103}Rh coupling with coupling constants typical of Rh(I) complexes ($J_{\text{RhPAN}_3} = 136.9 \text{ Hz}$; $J_{\text{RhPBz}_3} = 155.3 \text{ Hz}$) [23]. Magnetic inequivalence can also be observed from the ^1H NMR spectra of both complexes, which show the expected signals for the COD and the aromatic protons and broad signals for the benzyl CH_2 and OMe anisyl proton resonances.

The solution structure proposed for complexes **3** and **4** has been confirmed in the case of **4**, by X-ray crystallography, and the ORTEP diagram of such species is shown in Fig. 4. A summary of crystal data and a selection of bond distances (\AA) and angles ($^\circ$) are collected in Tables 1 and 2.

Complex **4** crystallizes in a triclinic system (space group P_{-1}), and exhibits a strongly distorted square planar geometry due to the presence of two *cis* disposed bulky phosphine ligands. Ir–P bond distances of ca. 2.35 \AA and 2.36 \AA were found for Ir–P(1) and Ir–P(2), respectively, which are similar to each other and in the range of distances found for this kind of complexes [20–22]. Also, the P(1)–Ir–P(2) angle is higher than 90° , due to steric repulsion between the bulky phosphine ligands [P(1)–Ir–P(2) = 94.7°].

Upon reaction with strong σ -donors such as pyridine and NH_4PF_6 , which contains the bulk and weakly coordinating hexafluorophosphate counterion in polar solvents, e.g. methanol, cationic complexes of formula $[\text{M}(\text{py})(\text{PAN}_3)(\text{COD})]^+$ (M = Rh, **5**; Ir, **6**) could be isolated as air and moisture stable solids. Complexes **5** and **6** are reminiscent of both the well-known Crabtree's catalyst $[\text{Ir}(\text{py})(\text{PCy}_3)(\text{COD})]\text{PF}_6$ [20] and the previously reported PBz_3 compounds $[\text{M}(\text{py})(\text{PBz}_3)(\text{COD})]\text{PF}_6$ (M = Rh; Ir) [18]. The two complexes were characterized by NMR spectroscopy and exhibit a fluxional behavior in solution at room temperature likely caused by the steric crowding at the metal center due to the presence of the bulky phosphine ligand PAN_3 . Raising the temperature to 50°C narrows the $^{31}\text{P}\{^1\text{H}\}$ NMR signals for both complexes, particularly for compound **5** where the doublet due to ^{103}Rh coupling ($J_{\text{RhP}} = 153.9 \text{ Hz}$), typical of a Rh(I) compound is clearly discernable [23].

2.3. Reaction of $[\text{IrCl}(\text{COD})]_2$ and PAN_3 with H_2

In an attempt to determine whether the coordination to iridium of two PAN_3 species was possible, the iridium dimer $[\text{IrCl}(\text{COD})]_2$ was treated with four equivalents of PAN_3 in a coordinating solvent such as acetone- d_6 (NMR-tube test). Only compound **2** was identified by $^{31}\text{P}\{^1\text{H}\}$ NMR spectroscopy. However, when a H_2

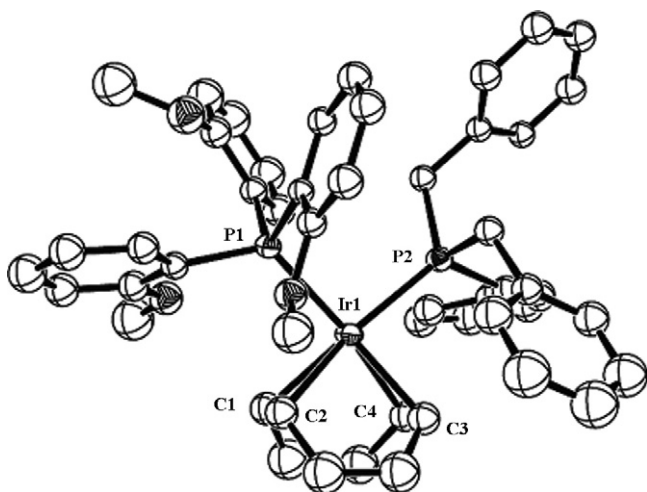
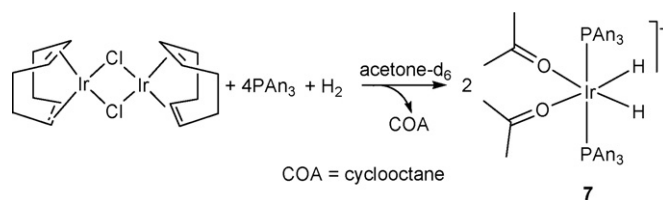
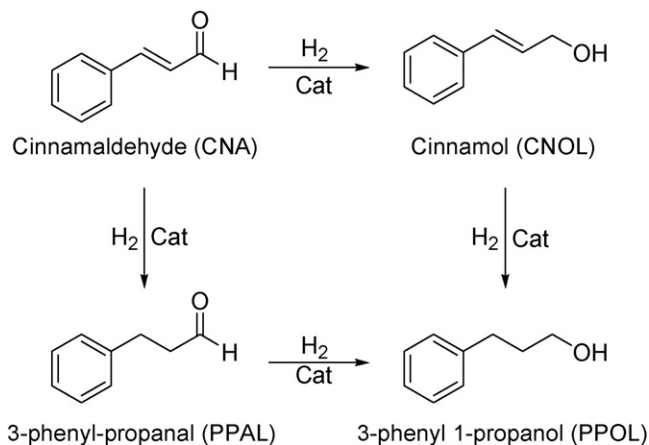


Fig. 4. ORTEP drawing of the complex $[\text{Ir}(\text{PBz}_3)(\text{PAN}_3)(\text{COD})]\text{PF}_6$ (**4**).



stream was passed through the solution cooled to ca. 0 °C, NMR signals ascribable to two new phosphine containing species could be identified. The first of them could be assigned to the bis(hydride)-bis(acetone)-bis(PAn₃) Ir(III) product [Ir(H)₂(acetone)₂(PAn₃)₂]PF₆ (**7**) (Scheme 3), analogous to other previously reported solvate dihydrides of tertiary phosphine ligands [18,24]. The other species (**8**) shows two doublets in the ³¹P{¹H} NMR (−32.5 and −40.1 ppm, *J*_{PP} = 43.2 Hz). Although the solution structure of complex **8** could not be unequivocally assigned, the experimental evidence suggests the presence of a chelating PAn₃ ligand, similar to that found for metal complexes of MDMPP, BDMPP or TDMPP ligands, in which the phosphine coordinates through both the phosphorous and one or more oxygen atoms [4]. Further evidence is required to substantiate this putative structural hypothesis.

2.4. Homogeneous hydrogenation of *trans*-cinnamaldehyde. Evaluation of iridium-bulky phosphine precursors

The selective hydrogenation of α,β-unsaturated aldehydes is an important process for the production of useful chemicals for the fragrance and pharmaceutical industries [25]. Several reports have appeared in which homogeneous [26], heterogeneous [27] and biphasic [28] systems have been tested, probing the importance of this reaction. It has been shown [26] that the catalytic synthesis of the saturated alcohol is favored, since it is easier to hydrogenate C=C double bonds compared to C=O aldehyde moieties [29]. A number of ruthenium and rhodium monophosphine complexes have shown good activities and variable selectivity [29] while their iridium counterparts generally show lower activities but better selectivities [30].

The expected catalytic hydrogenation pathway for *trans*-cinnamaldehyde (CNA) to the corresponding products, the saturated aldehyde 3-phenyl propanal (PPAL), the allylic alcohol cinnamol (CNOL), and the saturated alcohol 3-phenyl-1-propanol (PPOL) is shown in Scheme 4.

The screening of sterically hindered phosphine ligand complexes was carried out initially, using the known complex [Ir(py)(PBz₃)(COD)]PF₆ as catalyst precursor [18], which has been previously evaluated by some of us for the hydrogenation of imines [31]. The reaction conditions employed were: *T* = 80 °C; *p*_{H₂} = 17.1 bar and a catalyst load of 1 mol%. The reaction profile obtained is shown in Fig. 5. This catalyst precursor is able to convert CNA under the studied conditions, in moderate yields, to the following product distribution: 50.2% PPAL, 1.40% CNOL and 20.5% PPOL. No decarbonylation products were detected (e.g. allylbenzene), indicating that the system works exclusively for hydrogenation in our experimental conditions. This precursor reduces mainly the C=C moiety instead of the C=O bond, which would indicate that the saturated aldehyde (PPAL) is produced in a first stage followed by the C=O reduction of the aldehyde, to produce the saturated alcohol, PPOL. No decomposition of the catalyst precursor was observed and, in fact, the homogeneity of the reaction was proven through the mercury test [32].

The effect of the reaction temperature was also studied, with temperatures ranging between 40 °C and 100 °C. These results are summarized in Fig. 6. As can be observed, a rise in the reaction temperature promotes the conversion of the substrate, reaching a maximum yield of 96% at 100 °C. This linearity is confirmed since, at lower temperatures, the conversion decreases considerably, and at 40 °C, only 44% of the substrate is transformed.

However, it was also observed that rising the reaction temperature not only increases the amount of converted CNA, but also affects the product distribution. Figs. 7–9 show the effect of changing the reaction temperature on the yields and product distribution. From Fig. 7, we may conclude that the yield of PPAL increases progressively with the temperature. Below 100 °C, the production of

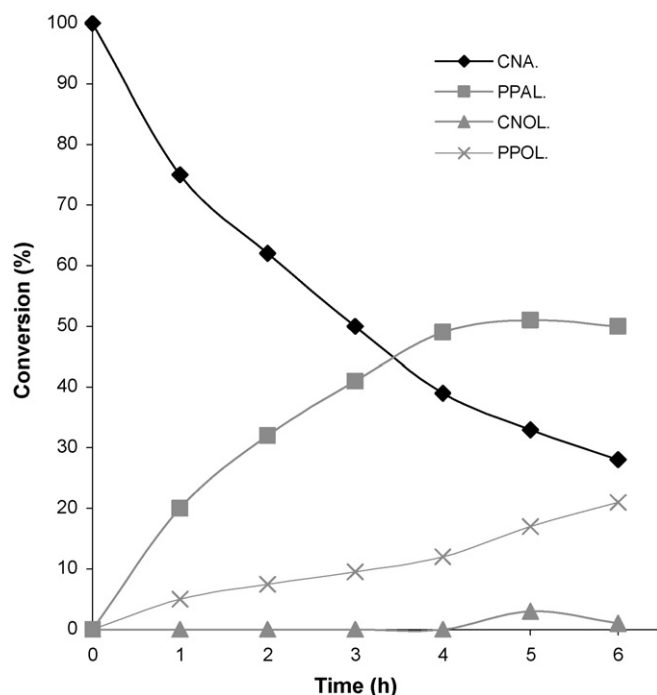


Fig. 5. Hydrogenation of *trans*-cinnamaldehyde using [Ir(py)(PBz₃)(COD)]PF₆ as catalyst precursor. *T* = 80 °C; *p*_{H₂} = 17.1 bar; catalyst = 1 mol%; toluene = 50 mL; time = 6 h.

PPAL reaches values in the range of 25–50% in 6 h. However, at 100 °C, a maximum yield of PPAL is obtained in 4 h (60%), followed by a decrease in the yield of this product, since the hydrogenation of the C=O moiety becomes more predominant. Therefore, a consecutive hydrogenation to yield PPAL followed by its transformation into PPOL is proposed.

The low yields of CNOL (Fig. 8) are not notably affected by the reaction temperature. For PPOL, the results displayed in Fig. 9 show

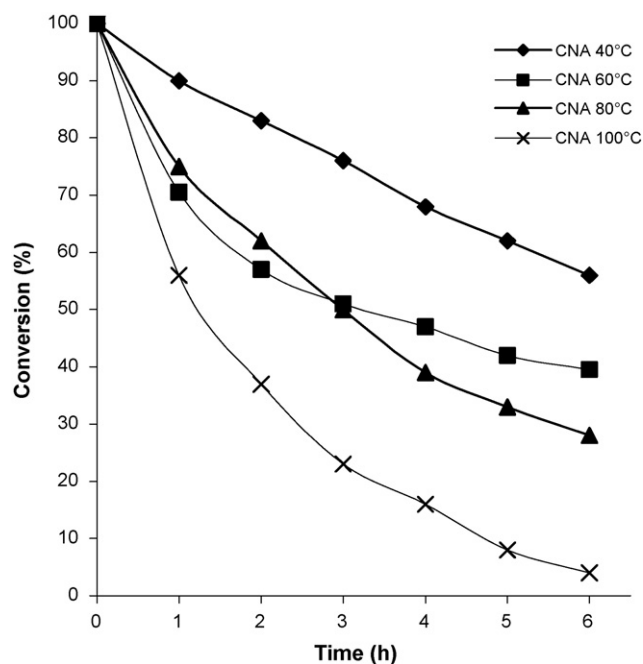


Fig. 6. Effect of the reaction temperature on the hydrogenation of *trans*-cinnamaldehyde using [Ir(py)(PBz₃)(COD)]PF₆ as catalyst precursor. *T* = 80 °C; *p*_{H₂} = 17.1 bar; catalyst = 1 mol%; toluene = 50 mL; time = 6 h.

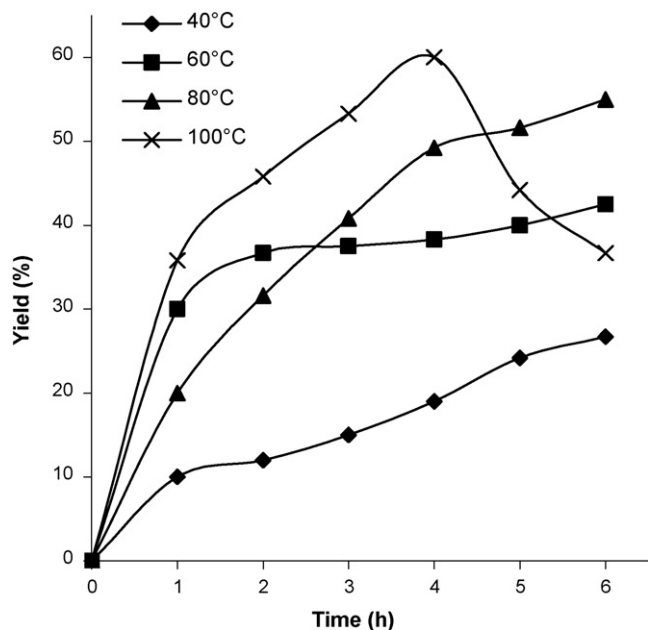


Fig. 7. Yield of 3-phenyl-propanal (PPAL) as a function of the reaction temperature in the hydrogenation of *trans*-cinnamaldehyde using $[\text{Ir}(\text{py})(\text{PBz}_3)(\text{COD})]\text{PF}_6$ as catalyst precursor. $T = 80^\circ\text{C}$; $\text{pH}_2 = 17.1$ bar; catalyst = 1 mol%; toluene = 50 mL; time = 6 h.

that the effect of the reaction temperature is more predominant at 100°C , achieving 52% conversion after 6 h of reaction. Below this temperature, there is practically no conversion to the saturated alcohol.

The effect of the hydrogen pressure was also studied. The conversion of CNA does not suffer practically any modification by varying the H_2 pressure. At 9.5 bar, 44% conversion is achieved, in comparison with 72.1% at 17.1 bar, and at 30.6 bar, only 52% of the substrate is transformed. In any case, C=C bond hydrogenation prevails over the reduction of the C=O moiety, indicating that modification of the

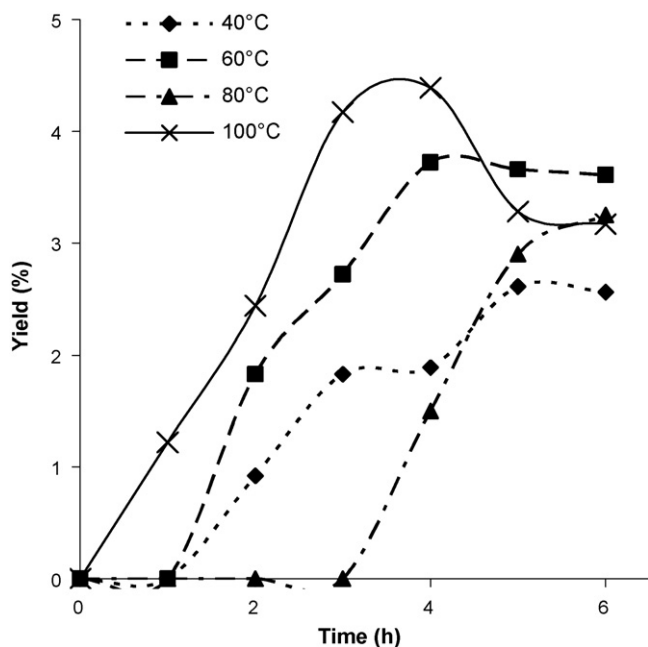


Fig. 8. Yield of cinnamol (CNOL) as a function of the reaction temperature in the hydrogenation of *trans*-cinnamaldehyde using $[\text{Ir}(\text{py})(\text{PBz}_3)(\text{COD})]\text{PF}_6$ as catalyst precursor. $T = 80^\circ\text{C}$; $\text{pH}_2 = 17.1$ bar; catalyst = 1 mol%; toluene = 50 mL; time = 6 h.

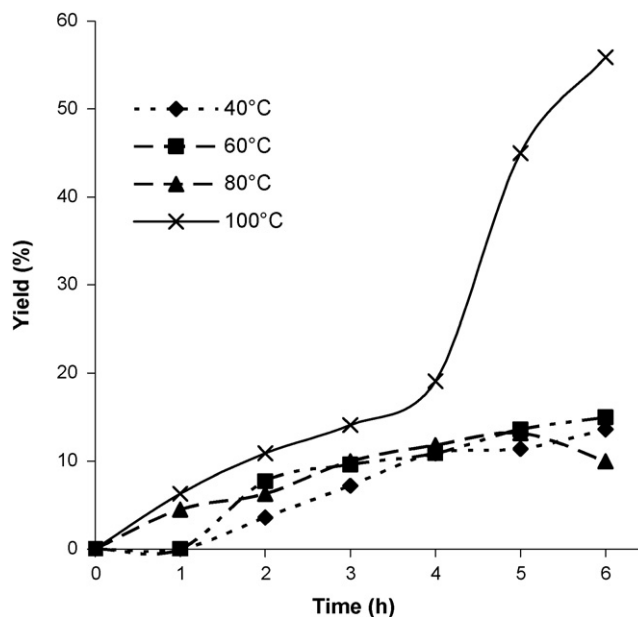


Fig. 9. Yield of 3-phenyl-1-propanol (PPOL) as a function of the reaction temperature in the hydrogenation of *trans*-cinnamaldehyde using $[\text{Ir}(\text{py})(\text{PBz}_3)(\text{COD})]\text{PF}_6$ as catalyst precursor. $T = 80^\circ\text{C}$; $\text{pH}_2 = 17.1$ bar; catalyst = 1 mol%; toluene = 50 mL; time = 6 h.

hydrogen pressure does not affect the selectivity or the rate of the conversion.

The effect of the substrate/catalyst ratio (S/C) on the conversion of CNA was also studied, and the results are summarized in Table 3. As can be observed, the conversion decreases from 87.2% to 28.0% as the substrate:catalyst ratio increases. The product distribution is also affected, showing that at low S/C ratios, the yield of PPAL is about 50.0%, while the production of the saturated alcohol PPOL reaches its maximum value of 36.4%. Furthermore, when the S/C ratio changes from 50 to 200 the major product is the saturated aldehyde PPAL and the production of PPOL decreases considerably. Finally, at the highest S/C ratio studied, the conversion decreases considerably, but the product distribution still favors the production of PPAL. Some changes in selectivity also occur, showing that the S/C ratio orients the C=C and C=O hydrogenation. At S/C ratios of 50 and 100, the hydrogenation of C=C double bond prevails over

Table 3
Effect of the catalyst load on the hydrogenation of *trans*-cinnamaldehyde using $[\text{Ir}(\text{py})(\text{PBz}_3)(\text{COD})]\text{PF}_6$ as catalyst precursor.

Entry	CNA:cat. ratio	Conversion (%)	Product distribution (%)			Selectivity PPAL/CNOL
			PPAL	CNOL	PPOL	
1	50	87.2	47.6	3.30	36.4	14.6
2	100	72.1	50.2	1.40	20.5	36.0
3	200	47.3	33.6	4.50	9.10	7.50
4	300	28.0	18.5	3.50	6.00	5.30

$T = 80^\circ\text{C}$; $\text{pH}_2 = 17.1$ bar; toluene = 50 mL; time = 6 h.

Table 4
Effect of the solvent on the hydrogenation of *trans*-cinnamaldehyde using $[\text{Ir}(\text{py})(\text{PBz}_3)(\text{COD})]\text{PF}_6$ as catalyst precursor.

Entry	Solvent	Product distribution (%)		
		PPAL	CNOL	PPOL
1	Toluene	50.2	1.40	20.5
2	THF	2.10	0.30	0.00
3	MeOH ^a	6.40	0.00	0.00

$T = 80^\circ\text{C}$; $\text{pH}_2 = 17.1$ bar; catalyst = 1 mol%; time = 6 h.

^a Slight decomposition observed.

Table 5Effect of the variation of the phosphine ligand in the hydrogenation of *trans*-cinnamaldehyde using $[\text{Ir}(\text{py})(\text{PAR}_3)(\text{COD})]\text{PF}_6$ as catalyst precursors.

Entry	Ar	Cone angle (θ)	Conversion (%)	Product distribution (%)			C=C/C=O ratio
				PPAL	CNOL	PPOL	
1	<i>o</i> -OCH ₃ C ₆ H ₄ ^a	194	99.5	57.5	1.40	41.1	10.3
2	-CH ₂ C ₆ H ₅	165	72.1	50.2	1.40	20.5	36.0
3	<i>o</i> -CH ₃ C ₆ H ₄	195	67.8	54.0	5.00	8.80	41.3

T = 80 °C; pH₂ = 17.1 bar; toluene = 50 mL; catalyst = 1 mol%; time = 6 h.^a Slight decomposition observed.

the C=O bond (entries 1 and 2). When this ratio increases to values of S/C of 200 or 300, C=O hydrogenation becomes more important. This suggests that the modification of the catalyst concentration can be used to modify the product selectivity in this reaction.

The effect of the solvent was also studied, using toluene, methanol and THF. The results are presented in Table 4. As can be observed, the solvent has a strong influence on the activity as well as in the product selectivity. In toluene 72.1% of conversion is achieved and the main product is the saturated aldehyde PPAL (entry 1). In THF (entry 2) the reaction is practically suppressed. Probably a THF ligand coordinates to the iridium center, blocking the vacant site required to coordinate the substrate during the hydrogenation step. In fact, mechanistic studies previously performed by some of us [18,31] indicate that under a H₂ stream a THF-*d*₈ solution of $[\text{Ir}(\text{COD})(\text{py})(\text{PBz}_3)]\text{PF}_6$ generates a dihydrido-solvento complex $[\text{Ir}(\text{H})_2(\text{THF})_2(\text{py})(\text{PBz}_3)]\text{PF}_6$. On the other hand, when MeOH is used, the conversion of CNA is close to 80.0% but the product analysis reveals that only 6.40% of the PPAL is produced and a new product, 1,1-dimethoxy-benzenepropane, is formed in 74.5%. This indicates that an acetalization of the aldehyde is promoted [33]. To figure out whether the metal complex leads to the formation of this new product, a blank experiment was carried out, showing that under these conditions, *trans*-cinnamaldehyde is the only product obtained. When the metal complex is present, it promotes C=C double bond hydrogenation, originating CNA. The absence of 1,1-dimethoxy-benzenepropane led us to the conclusion that the substrate is hydrogenated to CNA, which in a successive step reacts with MeOH to give the corresponding acetal.

A comparative study within the series of complexes $[\text{Ir}(\text{py})(\text{PAR}_3)(\text{COD})]\text{PF}_6$ (PAR₃ = PAN₃ (6); PBz₃ [18], PTol₃ [34]) has also been undertaken with the aim of studying the effect of phosphine ligands with variable steric and electronic characteristics [35]. These results are summarized in Table 5.

Replacing PBz₃ (cone angle 165°) with PAN₃, makes the conversion of CNA almost quantitative (entry 2 vs. entry 1), even though some catalyst decomposition was observed at the end of the reaction. Using PTol₃ (θ = 194°), slightly decreases the activity compared to the PBz₃ complex (entry 3 vs. entry 2). A change in selectivity is also observed. The PBz₃ compound hydrogenates the C=C bond 36 times more selectively than the C=O bond. With PTol₃, even if the steric hindrance at the metal center is high and comparable to that of PAN₃, the hydrogenation of CNA occurs, converting mainly the C=C double bond (C=C/C=O = 41.3) and practically all of the PPAL generated is transformed into the saturated alcohol PPOL. Confirmative evidence for assessing whether the steric hindrance is responsible for the selectivity towards the olefin can be addressed by using the PAN₃ complex. This system is selective also towards the C=C moiety, but the ratio C=C/C=O changes from 36 to 10.3, with a low production of the saturated alcohol PPOL, but a slightly higher yield of CNOL as compared to the PBz₃ and PTol₃ systems. These results suggest that a combination of electronic and steric properties of the phosphine ligands might be responsible for the changes in the activities and selectivities observed. Although sterically different, PBz₃ and PTol₃ are electronically very similar and this is probably associated with the C=C/C=O ratios obtained. PAN₃ being

a stronger base (pK_b = 4.47 [10b]) due to the presence of OCH₃ donor groups, has a different electronic character as compared to the other ligands used, explaining the lower C=C/C=O ratio obtained.

3. Conclusions

A new family of rhodium and iridium complexes with PAN₃ has been obtained. These complexes are straightforwardly prepared using simple procedures, and are air and moisture stable. A fluxional behavior in solution has been observed for all complexes due to the high steric hindrance at the metal centers, which was confirmed in the solid state by X-ray diffraction studies.

A screening of the hydrogenation reaction of cinnamaldehyde (CNA) was performed, using a series of cationic $[\text{Ir}(\text{py})(\text{PAR}_3)(\text{COD})]^+$ (PAR₃ = PAN₃, PBz₃, PTol₃) complexes indicating that all of the catalyst precursors preferentially hydrogenate the C=C double bonds instead of the C=O bond. Steric and electronic properties of the phosphine ligands in the iridium catalyst precursor have been found to influence both the activity and selectivity with the PAN₃ complex showing superior activity and C=C/C=O selectivity.

4. Experimental

4.1. General information

All reactions and manipulations were routinely performed under dry nitrogen or argon atmosphere using standard Schlenk techniques. ¹H and ¹³C{¹H} NMR spectra were recorded either on a Bruker ACP 200 (200.13 and 50.32 MHz), a Bruker AM 300 (300.13 and 75.47 MHz) or a Bruker Avance 500 (500.13 and 125.80 MHz) spectrometers. Peak positions are relative to tetramethylsilane and were calibrated against the residual solvent resonance (¹H) or the deuterated solvent multiplet (¹³C). ³¹P{¹H} NMR spectra were recorded on the same instruments operating at 81.01, 121.49, and 202.53 MHz, respectively. Chemical shifts were measured relative to external 85% H₃PO₄, with downfield shifts considered positive. All the NMR spectra were recorded at room temperature (25 °C) unless otherwise stated. Homonuclear decoupling experiments were carried out on a Bruker ACP 200 (200.13 MHz). Infrared spectra were recorded either on a PerkinElmer 1600 series or a Nicolet Magna IR 560 FT-IR spectrometers, using samples mullied in Nujol between KBr plates or in KBr disk. Elemental analyses (C, H, N) were performed using a Carlo Erba model 1106 elemental analyzer by the Microanalytical Service of the Department of Chemistry at the University of Florence (I). Reactions under controlled gas pressure were performed on Parr reactors.

4.2. Materials

Unless otherwise stated, all solvents were distilled just prior to use from appropriate drying agents. Methanol was distilled from Mg(OMe)₂, dichloromethane and acetonitrile from CaH₂, and tetrahydrofuran (THF) from sodium/benzophenone. Diethylether and petroleum ether were dried with sodium. Hydrogen was purified passing it through two columns in series

containing CuO/Al₂O₃ and CaSO₄, respectively. Deuterated solvents were dried over activated 4 Å molecular sieves prior to use. *Trans*-cinnamaldehyde (CNA) was purified by distillation under reduced pressure. All other chemicals were commercial products and used as received without further purification. Literature methods were employed for the synthesis of tris(*ortho*-anisyl)phosphine (PAN₃) [36], tribenzylphosphine (PBz₃) [18], [RhCl(COD)]₂ [37], [IrCl(COD)]₂ [38], [Ir(py)(PBz₃)(COD)]PF₆ [18], and [Ir(py)(PTol₃)(COD)]PF₆ [34]. A modification of the method reported in the literature [15], using dichloromethane as solvent and crystallizing from ethanol/dichloromethane, was followed for the synthesis of RhCl(PAN₃)(COD) (**1**), which led to an improved yield (90%), and the possibility to grow suitable crystals to perform X-ray diffraction. The solid complexes were collected on a sintered glass-frit and washed with ethanol and light petroleum ether (bp 40–60 °C) or *n*-pentane before being dried in a stream of nitrogen. GC–MS analyses were performed using a HP 5890 SERIES II PLUS with FI detector and a Megabore type capillary column, 15 m (DB-5 phase; 1.5 μm, J and W Scientific) with the following temperature program: 100 °C/3 min–10 °C/min–150 °C/6 min.

4.3. IrCl(PAN₃)(COD) (**2**)

[IrCl(COD)]₂ (500 mg; 0.74 mmol) and PAN₃ (540 mg; 1.50 mmol) were dissolved in dichloromethane (15 mL) and vigorously stirred for 30 min. Upon addition of ethanol and concentration, a yellow-orange solid precipitated. The solid was filtered off and washed with ethanol and *n*-pentane. Yield: 0.91 g; 89%. ¹H NMR (CDCl₃, 25 °C, 500.13 MHz): δ 1.57 (m, 4H, CH₂ COD); δ 1.69 (m, 4H, CH₂ COD); δ 2.18 (m, 2H, CH COD); δ 4.82 (br s, 2H, CH COD); δ 3.50 (s, 9H, –OCH₃); δ 6.86 (dd, 3H, aromatic); δ 6.97 (t, 3H, aromatic); δ 7.37 (t, 3H, aromatic); δ 7.72 (t, 3H, aromatic). ³¹P{¹H} NMR (CDCl₃, 25 °C, 121.5 MHz): δ 13.34 (s). IR (KBr): ν(Ir–Cl) 506 cm^{–1} (m). Anal. Calc. for C₂₉H₃₃PO₃ClIr: C, 50.61; H, 4.83. Found: C, 49.61; H, 4.73%.

4.4. [Rh(PAN₃)(PBz₃)(COD)]PF₆ (**3**)

An acetone solution of **1** (500 mg; 0.83 mmol) was treated with AgOSO₂CF₃ (290 mg; 1.78 mmol), under vigorous stirring for 30 min. The solution was filtered out and PBz₃ (280 mg; 0.92 mmol) was added, and the solution turned orange. NH₄PF₆ (275 mg; 1.69 mmol) and ethanol (20 mL) were added, and concentration under a brisk current of nitrogen precipitated a yellow solid, which after filtration was washed with ethanol and *n*-pentane, and vacuum dried. Yield: 750 mg; 89%. ¹H NMR (CD₂Cl₂, 25 °C, 300.13 MHz): δ 1.87 (m, 4H, CH₂ COD); δ 2.40 (m, 4H, CH₂ COD); δ 2.96 (br s, 3H, OCH₃ PAN₃); δ 3.50 (br s, 3H, OCH₃ PAN₃); δ 3.87 (d, 6H, CH₂ PBz₃, *J*_{HP} = 9.5 Hz); δ 3.94 (br s, 3H, OCH₃ PAN₃); δ 5.49 (br s, 4H, CH COD); δ 7.00–7.63 (m, 27H, aromatic). ³¹P{¹H} NMR (CD₂Cl₂, 25 °C, 202.5 MHz): 23.9 (br d, *J*_{RHP} = 155.3); δ –2.1 (br d, *J*_{RHP} = 136.9); δ –143.0 (sept, *J*_{PF} = 713).

4.5. [Ir(PAN₃)(PBz₃)(COD)]PF₆ (**4**)

An acetone solution of **2** (500 mg; 0.73 mmol) was treated with AgOSO₂CF₃ (200 mg; 0.77 mmol), under vigorous stirring for 30 min. The solution was filtered out and PBz₃ (240 mg; 0.79 mmol) was added. NH₄PF₆ (250 mg; 1.53 mmol) and ethanol (20 mL) were added, and concentration under a brisk current of nitrogen precipitated a shiny red solid, which after filtration was washed with ethanol and *n*-pentane, and vacuum dried. Yield: 650 mg; 81%. ¹H NMR (CD₂Cl₂, 25 °C, 300.13 MHz): δ 1.26 (m, 4H, CH₂ COD); δ 1.84 (br s, 3H, OCH₃ PAN₃); δ 2.20 (br s, 4H, CH₂ COD); δ 2.58 (br s, 3H, OCH₃ PAN₃); δ 2.84 (br s, 3H, OCH₃ PAN₃); δ 3.30 (br s, 6H, CH₂ PBz₃); δ 4.26 (br s, 4H, CH COD); δ 6.97–7.64 (m, 27H, aromatic).

³¹P{¹H} NMR (CD₂Cl₂, 25 °C, 202.5 MHz): δ 13.6 (br s); δ –10.8 (br s); δ –143.0 (sept, *J*_{PF} = 713).

4.6. [Rh(py)(PAN₃)(COD)]PF₆ (**5**)

A suspension of **1** (250 mg; 0.42 mmol) in methanol (20 mL), under stirring, was treated with an excess of pyridine (0.20 mL, 2.53 mmol) for 60 min. NH₄PF₆ (150 mg; 0.92 mmol) was added. Concentration under vacuum separated a yellow solid which after filtration was washed with water (5 mL), methanol (5 mL) and diethyl ether (5 mL). The solid was vacuum dried. Yield: 285 mg; 87%. ¹H NMR (CDCl₃, 50 °C, 300.13 MHz): δ 2.06 (d, 4H, CH₂ COD); δ 2.54 (br s, 4H, CH₂ COD); δ 3.58 (s, 9H, OCH₃ PAN₃); δ 4.03 (br s, 2H, CH COD); δ 4.54 (br s, 2H, CH COD); δ 6.86 (dd, 3H, aromatic PAN₃); δ 6.94 (t, 3H, aromatic PAN₃); δ 7.06 (t, 3H, aromatic PAN₃); δ 7.43 (m, 7H, aromatics PAN₃ and py); δ 8.30 (d, 2H, aromatic py). ³¹P{¹H} NMR (CDCl₃, 50 °C, 121.5 MHz): δ 12.25 (d, *J*_{RHP} = 153.9); δ –142.9 (sept, *J*_{PF} = 713).

4.7. [Ir(py)(PAN₃)(COD)]PF₆ (**6**)

A suspension of **2** (250 mg; 0.73 mmol) in methanol (20 mL), under stirring, was treated with an excess of pyridine (0.18 mL, 2.28 mmol) for 60 min. NH₄PF₆ (150 mg; 0.92 mmol) was added. Concentration under vacuum separated a shiny orange solid which after filtration was washed with water (5 mL), methanol (5 mL) and diethyl ether (5 mL). The solid was vacuum dried. Yield: 280 mg; 88%. ¹H NMR (CDCl₃, 25 °C, 300.13 MHz): δ 1.84 (br d, 4H, CH₂ COD); δ 2.34 (m, 4H, CH₂ COD); δ 3.44 (br s, 11H, 2H COD y 9H–OCH₃); δ 4.08 (br s, 2H, CH COD); δ 6.78 (br s, 3H, aromatic PAN₃); δ 6.99 (br s, 3H, aromatic PAN₃); δ 7.17 (t, 3H, aromatic PAN₃); δ 7.40 (t, 4H, aromatic PAN₃ and py); δ 7.54 (td, 2H, aromatic py); δ 8.27 (d, 2H, aromatic py). ¹³C{¹H} NMR (CDCl₃, 25 °C, 75.5 MHz): δ 29.4 (CH₂ COD); δ 31.7 (CH₂ COD); δ 54.8 (–OCH₃); δ 66.9 (CH COD *trans* to py); δ 85.3 (d, CH COD *trans* to P); δ 111.0 (CH aromatic); δ 116.0 (C aromatic); δ 120.4 (d, CH, aromatic *ipso*, *J*_{CP} = 10.5 Hz); δ 124.9 (CH aromatics); δ 132.4 (CH aromatic); δ 135.6 (C aromatic); δ 137.1 (CH *para* py); δ 150.0 (CH *meta* py); δ 159.7 (CH *ortho* py). ³¹P{¹H} NMR (CDCl₃, 25 °C, 121.5 MHz): 9.63 (s); –143.03 (sept, *J*_{PF} = 712).

4.8. *In situ* reaction of [IrCl(COD)]₂ with PAN₃ and H₂ in acetone-*d*₆

[IrCl(COD)]₂ (30 mg; 0.045 mmol) and PAN₃ (33 mg; 0.094 mmol) were dissolved in acetone-*d*₆ (1 mL) and the solution was introduced into a 5 mm NMR tube under an inert atmosphere. After the tube was cooled to 0 °C, H₂ was gently bubbled into the solution for 5 min. ¹H and ³¹P{¹H} NMR spectra showed the formation of [Ir(H)₂(acetone)₂(PAN₃)₂]⁺ (**7**). All our attempts to isolate **7** by scaling up the reaction were unsuccessful. In all cases, products without hydride ligands or a mixture of unidentified products were obtained.

4.8.1. Selected NMR data for **7**

¹H NMR (acetone-*d*₆, 0 °C, 200.13 MHz): δ –31.6 (t, hydrides, *J*_{HP} = 16.0 Hz). ³¹P{¹H} NMR (acetone-*d*₆, 0 °C, 81.01 MHz): δ 17.93 (s).

4.9. X-ray diffraction studies

Summary of crystal data and structure refinement parameters for RhCl(PAN₃)(COD) (**1**) and [Ir(PBz₃)(PAN₃)(COD)]PF₆ (**4**) are reported in Table 1. Selected distances and angles for both compounds are summarized in Table 2.

4.9.1. $RhCl(PAn_3)(COD)$ (**1**)

Crystallographic data for **1** were collected on a CAD4 diffractometer using graphite monochromated Mo $K\alpha$ radiation ($\lambda = 0.7107 \text{ \AA}$) at room temperature. A set of 25 carefully centered reflections in the range $7^\circ < \theta < 9^\circ$ was used for determining the lattice constants. As a general procedure, the intensity of three standard reflections were measured periodically every 200 reflections for orientation and intensity control. This procedure revealed an 8% decay of intensities during the data collection period, for which the intensities were corrected. The data were corrected for Lorentz and polarization effects. Atomic scattering factors were those tabulated by Cromer and Waber [39] with anomalous dispersion corrections taken from reference [40]. An empirical absorption correction was applied via ψ scan with correction factors in the range 0.8401–0.8977. The computational work was carried out using the program SHELX97 [41]. All non-hydrogen atoms were refined with anisotropic displacement parameters (adps). Hydrogens atoms were geometrically placed and allowed to ride on their parent C atom with $U_{iso}(H) = 1.2U_{eq}(C)$. Idealized C–H distances were fixed at 0.93 Å (for C–H in phenyl groups), 0.97 Å (for C–H in CH_2 groups) and 0.98 Å (C–H in the 1,5-cyclo-octadiene group).

4.9.2. $[Ir(PBz_3)(PAn_3)(COD)]PF_6$ (**4**)

Crystallographic data for **4** were collected on a CAD4 diffractometer using graphite monochromated Mo $K\alpha$ radiation ($\lambda = 0.7107 \text{ \AA}$) at room temperature. A set of 25 carefully centered reflections in the range $7^\circ < \theta < 9^\circ$ was used for determining the lattice constants. As a general procedure, the intensity of three standard reflections were measured periodically every 200 reflections for orientation and intensity control. This procedure revealed a 7% decay of intensities during the data collection period, for which the intensities were corrected. The data were corrected for Lorentz and polarization effects. Atomic scattering factors were those tabulated by Cromer and Waber [39] with anomalous dispersion corrections taken from reference [40]. An empirical absorption correction was applied via ψ scan with correction factors in the range 0.8401–0.8977. The computational work was carried out using the program SHELX97 [41]. All non-hydrogen atoms were refined with anisotropic displacement parameters (adps). Hydrogens atoms were geometrically placed and refined following the same procedure described above for the Rh complex (**1**).

Crystallographic data for the structures in this paper have been deposited with the Cambridge Crystallographic Data Centre as numbers CCDC 701963 and CCDC 701964. Those contain the supplementary crystallographic data for this paper. These data can be obtained free of charge from The Cambridge Crystallographic Data Centre via www.ccdc.cam.ac.uk/data_request/cif.

4.10. Catalytic tests

In a typical experiment the catalyst precursor (0.024 mmol) and the substrate (2.4 mmol) were dissolved in toluene (50 mL) and introduced into a glass-lined stainless steel autoclave (300 mL) from a PARR instrument equipped with internal stirring, temperature control unit and a sampling valve. Air was removed by flushing three times with hydrogen and the reactor was charged to the required pressure (17.1 bar), heated to the reaction temperature (80 °C) under constant stirring at 430 rpm. During the catalytic test, the total pressure of the system was continuously adjusted to a constant value by making up from a high-pressure reservoir and reaction mixture samples were periodically taken through the sampling valve. The reaction was stopped after 6 h, and the reaction mixture was analyzed by gas chromatography. All catalytic results are the average of three consecutive experiments. The ratio of conversion is defined as: %conversion = (moles of product/moles of *trans*-cinnamaldehyde used) \times 100%.

Acknowledgements

The authors thank FONACIT (Venezuela) for financial support to V.L. (Ph.D. Fellowship and Project S3), FONACIT and CNR (Italy) for an International Cooperation Grant. We also thank Mr. Dante Masi (CNR) for collecting the X-ray diffraction data.

References

- [1] G. Gioia-Lobbia, C. Pettinari, C. Santini, M. Pelli, G. Valle, S. Calogero, *Inorg. Chem.* 37 (1998) 890–900.
- [2] H. Reinius, A. Krause, *Catal. Lett.* 70 (2000) 149–154.
- [3] L.J. Baker, R. Bott, G. Bowmaker, P. Healy, B. Skelton, P. Schwerdtfeger, A. White, *J. Chem. Soc., Dalton Trans.* (1995) 1341–1347.
- [4] For references on the chemistry of MDMPP, BDMPP or TDMPP, see:
 - (a) Y. Yamamoto, R. Sato, M. Ohshima, F. Matsuo, C. Sudoh, *J. Organomet. Chem.* 489 (1995) C68–C70;
 - (b) Y. Yamamoto, R. Sato, F. Matsuo, C. Sudoh, I. Toshiaki, *Inorg. Chem.* 35 (1996) 2329–2336;
 - (c) Y. Yamamoto, F. Arima, *J. Chem. Soc., Dalton Trans.* (1996) 1815–1821;
 - (d) Y. Yamamoto, T. Tomoaki, C. Sudoh, T. Tatsuhiro, *J. Organomet. Chem.* 569 (1998) 29–37;
 - (e) X. Han, Y. Yamamoto, *J. Organomet. Chem.* 561 (1998) 157–165;
 - (f) Y. Yamamoto, K. Sugawara, T. Aiko, J. Ma, *J. Chem. Soc., Dalton Trans.* (1999) 4003–4008;
 - (g) Y. Yamamoto, X. Han, H. Sugawara, A. Nishimue, *Angew. Chem. Int. Ed.* 38 (1999) 1242–1244;
 - (h) Y. Yamamoto, K. Kawasaki, S. Nishimura, *J. Organomet. Chem.* 587 (1999) 49–57;
 - (i) Y. Yamamoto, X. Han, J. Ma, *Angew. Chem. Int. Ed.* 39 (2000) 1965–1968;
 - (j) J. Ma, Y. Kojima, Y. Yamamoto, *J. Organomet. Chem.* 616 (2000) 149–156;
 - (k) Y. Yamamoto, X. Hang, S. Nishimura, K. Sugawara, N. Nezu, T. Tanase, *Organometallics* 20 (2001) 266–272;
 - (l) Y. Yamamoto, K. Sugawara, X. Han, *J. Chem. Soc., Dalton Trans.* (2002) 195–211;
 - (m) Y. Yamamoto, K. Sugawara, M. Kakeya, *Inorg. Chim. Acta* 340 (2002) 21–28;
 - (n) Y. Yamamoto, J. Seta, H. Murooka, X. Han, *Inorg. Chem. Commun.* 6 (2003) 202–205;
 - (o) Y. Yamamoto, Y. Kosaka, Y. Tsutsumi, Y. Sunada, K. Tatsumi, T. Fumie, T. Shigetoshi, *Dalton Trans.* (2004) 2969–2978;
 - (p) Y. Yamamoto, A. Takahashi, Y. Sunada, K. Tatsumi, *Inorg. Chim. Acta* 357 (2004) 2833–2840.
- [5] (a) N.A. Bell, S.J. Coles, M.B. Hursthouse, M.E. Light, K.A. Malik, R. Mansor, *Polyhedron* 19 (2000) 1719–1726;
- (b) J. Yang, G.J. Mercer, H.M. Nguyen, *Org. Lett.* 9 (2007) 4231–4234.
- [6] For references on the chemistry of TMPP, see:
 - (a) K.R. Dunbar, S. Haefner, L. Pence, *J. Am. Chem. Soc.* 111 (1989) 5504–5506;
 - (b) K.R. Dunbar, S. Haefner, A. Quillevéré, *Polyhedron* 9 (1990) 1695–1702;
 - (c) S. Chen, K.R. Dunbar, *Inorg. Chem.* 29 (1990) 588–590;
 - (d) K.R. Dunbar, S. Haefner, D. Burzynsky, *Organometallics* 9 (1990) 1347–1349;
 - (e) K.R. Dunbar, L. Pence, *Acta Crystallogr. C47* (1991) 23–26;
 - (f) K.R. Dunbar, A. Quillevéré, S. Haefner, *Acta Crystallogr. C47* (1991) 2319–2321;
 - (g) S. Chen, K.R. Dunbar, *Inorg. Chem.* 30 (1991) 2018–2023;
 - (h) S. Haefner, K.R. Dunbar, C. Bender, *J. Am. Chem. Soc.* 113 (1991) 9540–9553;
 - (i) K.R. Dunbar, S. Haefner, *Organometallics* 11 (1992) 1431–1433;
 - (j) K.R. Dunbar, *Commun. Inorg. Chem.* 13 (1992) 313–357;
 - (k) K.R. Dunbar, A. Quillevéré, *Organometallics* 12 (1993) 618–620;
 - (l) K.R. Dunbar, A. Quillevéré, *Polyhedron* 12 (1993) 807–819;
 - (m) K.R. Dunbar, J. Matonic, V. Saharan, *Inorg. Chem.* 33 (1994) 25–31;
 - (n) K.R. Dunbar, S. Haefner, C. Uzelmeier, A. Howard, *Inorg. Chim. Acta* 240 (1995) 527–534;
 - (o) J. Sun, C. Uzelmeier, D.L. Ward, K.R. Dunbar, *Polyhedron* 17 (1998) 2049–2063;
 - (p) J. Sun, H. Zhao, X. Ouyang, R. Clérac, J.A. Smith, J.M. Clemente-Juan, C. Gómez-García, E. Coronado, K.R. Dunbar, *Inorg. Chem.* 38 (1999) 5841–5855.
- [7] (a) T. Schmidt, Z. Dai, H. Drexler, W. Baumann, C. Jaeger, D. Pfeifer, D. Heller, *Chem. Eur. J.* 14 (2008) 4469–4471;
- (b) Y. Wada, T. Imamoto, H. Tsuruta, K. Yamaguchi, I.D. Gridnev, *Adv. Synth. Catal.* 346 (2004) 777–788 (and references therein).
- [8] (a) C.C. Pai, C.W. Lin, C.C. Chen, A. Chan, *J. Am. Chem. Soc.* 122 (2000) 11513–11514;
- (b) L.J. Higham, E.F. Clarke, H. Müller-Bunz, D.G. Gilheany, *J. Organomet. Chem.* 690 (2005) 211–219;
- (c) P. Sauvageot, O. Blacque, M.M. Kubicki, S. Jugé, C. Moise, *Organometallics* 15 (1996) 2399–2403.
- [9] (a) H. Gulyás, Z. Bacsik, Á. Szöllösy, J. Bakos, *Adv. Synth. Catal.* 348 (2006) 1306–1310;
- (b) J. Vela, G.R. Lief, Z. Shen, R.F. Jordan, *Organometallics* 26 (2007) 6624–6635;
- (c) S. Liu, S. Borkar, D. Newsham, H. Yennawar, A. Sen, *Organometallics* 26 (2007) 210–216.
- [10] (a) Y. Yamashoji, T. Matsushita, M. Wada, T. Shono, *Chem. Lett.* 17 (1987) 43–46;
- (b) Y. Yamashoji, T. Matsushita, M. Tanaka, T. Shono, M. Wada, *Polyhedron* 8 (1989) 1053–1059.

- [11] N.A. Barnes, S.M. Godfrey, R.T.A. Halton, I. Mushtaq, R.G. Pritchard, *Dalton Trans.* (2006) 4795–4804.
- [12] H.C. Aspinall, M.R. Tillotson, *Inorg. Chem.* 35 (1996) 5–8.
- [13] L. Hirsivaara, L. Guericcaibetia, M. Haukka, P. Suomalainen, R.H. Laitinen, T.A. Pakkanen, J. Pursiainen, *Inorg. Chim. Acta* 307 (2000) 48–57.
- [14] (a) S.S. Gunatilleke, A.M. Barrios, *J. Med. Chem.* 49 (2006) 3933–3937; (b) R.C. Bott, P.C. Healy, G. Smith, *Polyhedron* 26 (2007) 2803–2809.
- [15] J. Tiburcio, S. Bernès, H. Torrens, *Polyhedron* 25 (2006) 1549–1554.
- [16] F.P. Pruchnik, R. Starosta, M.W. Kowalska, E. Gałdecka, Z. Gałdecki, A. Kowalski, *J. Organomet. Chem.* 597 (2000) 20–28.
- [17] M. Bartók, Á. Molnár, *The Chemistry of Double-Bonded Functional Group, Supplement A3*, Wiley, New York, 1997, p. 843.
- [18] V.R. Landaeta, M. Peruzzini, V. Herrera, C. Bianchini, R.A. Sánchez-Delgado, A.E. Goeta, F. Zanobini, *J. Organomet. Chem.* 691 (2006) 1039–1050.
- [19] For references on related MCl(P)(cod) (M = Rh, Ir; P = tertiary phosphine ligand) compounds, see:
(a) A.M. Slawin, M.B. Smith, D. Woollins, *J. Chem. Soc., Dalton Trans.* (1996) 1283–1293;
(b) J. Ho Shin, B.M. Bridgewater, D.G. Churchill, G. Parkin, *Inorg. Chem.* 40 (2001) 5626–5635;
(c) C.M. Thomas, R. Mafua, B. Therrien, E. Rusanov, H. Stoeckli-Evans, G. Süß-Fink, *Chem. Eur. J.* 8 (2002) 3343–3352.
- [20] (a) R.H. Crabtree, G.E. Morris, *J. Organomet. Chem.* 135 (1977) 395–403; (b) R.H. Crabtree, A. Gautier, G. Giordano, T. Khan, *J. Organomet. Chem.* 141 (1977) 113–121; (c) R.H. Crabtree, *Acc. Chem. Res.* 12 (1979) 331–337.
- [21] (a) L. Haines, *Inorg. Nucl. Chem. Lett.* 5 (1969) 399–403; (b) L. Haines, *Inorg. Chem.* 9 (1970) 1517–1520; (c) R. Haszeldine, R. Lunt, R. Parish, *J. Chem. Soc. A* (1971) 3705–3711; (d) W.J. Suggs, S.D. Cox, R.H. Crabtree, *J.M. Quirk, Tetrahedron Lett.* 22 (1981) 303–306; (e) R.H. Crabtree, *Chem. Rev.* 85 (1985) 245–269.
- [22] (a) L.M. Haines, E. Singleton, *J. Chem. Soc., Dalton Trans.* (1972) 1891–1896; (b) J.R. Shapley, R.R. Schrock, J.A. Osborn, *J. Am. Chem. Soc.* 91 (1969) 2816–2817; (c) R. Schrock, J.A. Osborn, *J. Am. Chem. Soc.* 93 (1971) 2397–2407; (d) R. Usón, L.A. Oro, M.J. Fernández, *J. Organomet. Chem.* 193 (1980) 127–133.
- [23] C. Bianchini, D. Masi, A. Meli, M. Peruzzini, F. Zanobini, *J. Am. Chem. Soc.* 110 (1988) 6411–6423.
- [24] R.H. Crabtree, P.C. Demou, D. Eden, J.M. Mihelcic, C.A. Parnell, J.M. Quirk, G.E. Morris, *J. Am. Chem. Soc.* 104 (1982) 6994–7001.
- [25] (a) P. Gallezot, D. Richard, *Catl. Rev.-Sci. Eng.* 40 (1998) 81; (b) P. Clauss, *Top. Catal.* 5 (1998) 51; (c) R.L. Augustine, *Heterogeneous Catalysis for Organic Synthesis*, Dekker, New York, 1995; (d) K. Bauer, D. Garbe, *Common Fragrance and Flavor Materials*, VCH, Weinheim, 1985; (e) K. Weissmermel, H.J. Arpe, *Industrial Organic Chemistry*, Verlag, Chemie, Weinheim, 1978.
- [26] Some reports on the homogeneous hydrogenation of cinnamaldehyde are:
(a) C.A. Mebi, R.P. Nair, B.J. Frost, *Organometallics* 26 (2007) 429–438; (b) P. Csabai, F. Joó, *Organometallics* 23 (2004) 5640–5643; (c) D. Darensbourg, F. Joó, M. Kannisto, A. Kathó, J.H. Reibenspies, *Organometallics* 11 (1992) 1990–1993; (d) A. Rossin, G. Kovács, G. Ujaque, A. Lledós, F. Joó, *Organometallics* 25 (2006) 5010–5023.
- [27] Some reports on the heterogeneous hydrogenation of cinnamaldehyde are:
(a) M.L. Toebe, F.F. Prinsloo, J.H. Bitter, A.J. van Dillen, K.P. de Jong, *J. Catal.* 214 (2003) 78–87; (b) S. Fujita, S. Akihara, F. Zhao, R. Liu, M. Hasegawa, M. Arai, *J. Catal.* 236 (2005) 101–111; (c) G.R. Cairns, R.J. Cross, D. Stirling, *J. Catal.* 166 (1997) 89–97; (d) C. Pham-Huu, N. Keller, G. Ehret, L.J. Charbonniere, R. Ziesel, M.J. Ledoux, *J. Mol. Catal.* 170 (2001) 155–163; (e) H. Li, X. Chen, M. Wang, Y. Xu, *Appl. Catal.* 225 (2002) 117–130; (f) J. Tessonnier, L. Pesant, G. Ehret, M.J. Ledoux, C. Pham-Huu, *Appl. Catal.* 288 (2005) 203–210; (g) S. Fujita, S. Akihara, M. Arai, *J. Mol. Catal.* 249 (2006) 223–229.
- [28] Some reports on the biphasic hydrogenation of cinnamaldehyde are:
(a) A. Andriollo, J. Carrasquel, J. Mariño, F.A. López, D.E. Páez, I. Rojas, N. Valencia, *J. Mol. Catal.* 116 (1997) 157–165; (b) R.A. Sánchez-Delgado, M. Medina, F. López-Linares, A. Fuentes, *J. Mol. Catal.* 116 (1997) 167–177; (c) F. López-Linares, M.G. González, D.E. Páez, *J. Mol. Catal.* 145 (1999) 61–68; (d) S. Bolaño, L. Gonsalvi, F. Zanobini, F. Vizza, V. Bertolasi, A. Romerosa, M. Peruzzini, *J. Mol. Catal.* 224 (2004) 61–70; (e) D. Darensbourg, N.W. Stafford, F. Joo, J.H. Reibenspies, *J. Organomet. Chem.* 488 (1995) 99–108; (f) K. Tin, N. Wong, R. Li, Y. Li, J. Hu, X. Li, *J. Mol. Catal.* 137 (1999) 121–125.
- [29] (a) B.R. James, A. Pacheco, S.J. Rettig, I.S. Thorburn, R.G. Ball, J.A. Ibers, *J. Mol. Catal.* 41 (1987) 147–161; (b) R. Noyori, H. Takaya, *Acc. Chem. Res.* 23 (1990) 345–350; (c) A. Mezzetti, G. Consiglio, *J. Chem. Soc., Chem. Commun.* (1991) 1675–1676; (d) S.A. King, S.A. Thompson, K.O. King, T.R. Verhoeven, *J. Org. Chem.* 57 (1992) 6689–6691; (e) R.X. Li, K.C. Tin, N.B. Wong, Z.Y. Zhang, T.C.W. Mak, X.J. Li, *J. Organomet. Chem.* 557 (1998) 207–212; (f) R.X. Li, N.B. Wong, X.J. Li, T.C.W. Mak, Q.C. Yang, K.C. Tin, *J. Organomet. Chem.* 571 (1998) 223–229; (g) A.S.C. Chan, W. Hu, C.C. Pai, C.P. Lau, Y. Jiang, A. Mi, M. Yan, J. Sun, R. Lou, J. Deng, *J. Am. Chem. Soc.* 119 (1997) 9570–9571.
- [30] (a) E. Farnetti, M. Pesce, J. Kaspar, R. Spogliarich, M. Graziani, *J. Chem. Soc., Chem. Commun.* (1986) 746–747; (b) E. Farnetti, G. Nardin, M. Graziani, *J. Organomet. Chem.* 417 (1991) 163–172; (c) E. Farnetti, J. Kaspar, R. Spogliarich, M. Graziani, *J. Chem. Soc., Dalton Trans.* (1988) 947–952; (d) R. Spogliarich, E. Farnetti, J. Kaspar, M. Graziani, *J. Mol. Catal.* 50 (1989) 19–29; (e) K. Mashima, T. Akutagawa, X. Zhang, H. Takaya, T. Taketomi, H. Kumobayashi, H. Akutagawa, *J. Organomet. Chem.* 428 (1992) 213–222; (f) B. James, R. Morris, *J. Chem. Soc., Chem. Commun.* (1978) 929–930; (g) W. Strohmeier, H. Steigerwald, *J. Organomet. Chem.* 129 (1997) C43–C46; (h) C.S. Chin, B. Lee, S.C. Park, *J. Organomet. Chem.* 393 (1990) 131–135.
- [31] V.R. Landaeta, B.K. Muñoz, M. Peruzzini, V. Herrera, C. Bianchini, R.A. Sánchez-Delgado, *Organometallics* 25 (2006) 403–409.
- [32] (a) D.R. Anton, R.H. Crabtree, *Organometallics* 2 (1983) 855–859; (b) Y. Lyn, R.G. Finke, *Inorg. Chem.* 33 (1994) 4891–4910.
- [33] J. Clayden, N. Greeves, S. Warren, P. Wothers, *Organic Chemistry*, Oxford University Press, New York, 2001 (Chapter 14, p. 342).
- [34] The analogue complex [Ir(COD)(py)(PTol₃)]PF₆ (Tol = *o*-CH₃C₆H₄) was synthesized according to the method described in [18] for PBz₃.
- [35] C.A. Tolman, *Chem. Rev.* 77 (1977) 313–348.
- [36] L. Brandsma, H.D. Verkruisje, *Synth. Commun.* 20 (1990) 2273–2274.
- [37] J. Chatt, L.M. Venanzi, *J. Chem. Soc.* (1957) 4735–4741.
- [38] J.L. Herde, J.C. Lambert, C.V. Senoff, *Inorg. Synth.* 15 (1974) 18–20.
- [39] D.T. Cromer, J.T. Waber, *Acta Crystallogr.* 18 (1965) 104–109.
- [40] *International Tables of Crystallography*, vol. IV, Kynoch Press, Birmingham, UK, 1974.
- [41] G.M. Sheldrick, SHEXL-97 (Release 97-2): Program for Structure Refinement, University of Göttingen, Göttingen, Germany, 1997.